Process-based Empirical Prediction of Landslides in Weakly Lithified Coastal Cliffs, San Francisco, California, USA

B.D. Collins & R. Kayen
United States Geological Survey, Western Coastal and Marine Geology, Menlo Park, California, USA

N. Sitar
University of California, Berkeley, Dept. of Civil and Envir. Engineering, Berkeley, California, USA

ABSTRACT: Coastal landslides in weakly lithified sediment are a common occurrence in many parts of the world, including the west coast of the United States. Here, geologically young (Quaternary), marine terrace deposits form steep, near vertical cliff exposures up to 30 m in height and extend for many kilometers along the coastlines of the states of California, Oregon, and Washington. A comprehensive research study begun in 2001 documented and monitored the effects of winter storms on several sections of cliff south of San Francisco, California, USA. We present the results of five seasons (2001-2006) of weekly observations of these cliffs, documenting failure occurrences, modes, and mechanisms along a 1.5 km stretch of coast, and correlate these with storm event precipitation totals and storm-induced ocean wave run-up heights. We utilize the results of the correlations to outline thresholds for the likelihood of cliff failure in order to form a process-based, short-term, methodology for landslide prediction. The methodology is generalized for long-term (decadal) predictions of landslide occurrence based on rates of sea-level rise, and possible changes in precipitation.

1 INTRODUCTION

Landslide and erosional failure of weakly lithified coastal cliffs (coastal bluffs or seacliffs) are a common occurrence along many of the world's coastlines. Whether composed of weakly cemented sands, nominally cohesive clays, or weaker bedrock members such as chalk, these lithologies form dynamic geomorphologic landscapes, especially when exposed to a suite of coastal and storm processes. Increasing development along these landscapes has been an inevitability in many parts of the world, including the west coast of the United States. In some locations, such as near the city of San Francisco, California, coastal cliffs and bluffs composed of weakly to moderately cemented sand have undergone continuous residential development for the past 50 years (Fig. 1). In many of these locations, initial coastal setback limits have either not been adequate or were never planned for, and residences and public utilities have been lost to coastal cliff retreat.

Given the continuous force of winter storms along this stretch of coast and climatic predictions of global warming and resulting sea-level rise (CCCC, 2006), cliff failures will be an inevitability for the foreseeable future, as will the associated catastrophic loss of property and potentially lives. There is therefore a need to predict future occurrences of cliff failures given projected sea-level, wave action, and precipitation trends.

In this paper, we develop empirical correlations for predicting cliff failure along a 1.5 km stretch of coastal cliff located in the city of Pacifica, California. While much research has focused on these cliffs due to their high failure rate (Clough et al. 1981, Hampton & Dingler, 1998, Lajoie & Mathieson, 1998, Hampton, 2002, Sallenger et al. 2002, Sitar, 1983, Snell et al. 2002), this study presents the first work aimed at systematically establishing the wave and precipitation scenarios that lead to cliff failure. The methodology relies on five years of direct observations of coastal cliff failures, and pairs these observations with high resolution records of coastal tides, open ocean wave heights, and precipitation records. The empirical correlations are modeled after existing methodologies for landslide occurrence dependent on cumulative seasonal rainfall (e.g. Nilsen et al. 1976) and rainfall intensity-duration thresholds (e.g. Caine, 1980; Cannon, S.H., 1988). While the effect of precipitation on seepage driven failures in moderately cemented coastal cliffs is handled in much the same way as existing correlations, we introduce a new methodology for identifying these thresholds for the effect of wave action on more weakly cemented cliffs.

Figure 1. Typical weakly lithified coastal cliffs with nearby residential development, Pacifica, California, USA

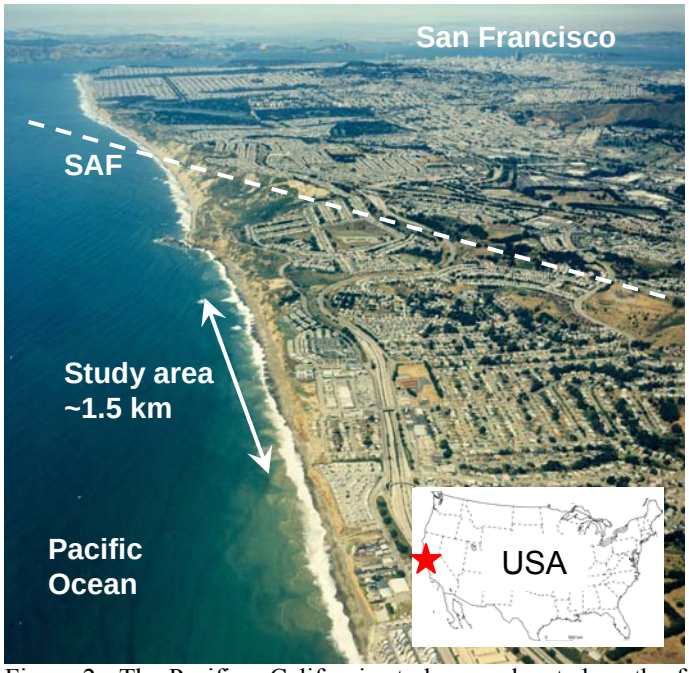

Figure 2. The Pacifica, California study area, located south of the San Andreas Fault zone (SAF).

2 REGIONAL SETTING

The Pacifica coastline extends for several kilometers along a tectonically active portion of the California coast, south of the city of San Francisco (Fig. 2). Located immediately south of the Mussel Rock splay of the San Andreas Fault zone, the geology of the area consists of elevated marine terraces composed of variably lithified Holocene beach and dune deposits and Pleistocene alluvial deposits. These terrace deposits overlay older, Mesozoic Franciscan bedrock members that are intermittently exposed at beach level and form small headlands between the currently eroding marine terrace deposits. Deposition of the terrace deposits occurred prior to the relative sea level fall in the area approximately 5000 years ago and which resulted in the uplifted, steep exposures of coastal cliff now present (Cleveland, 1975). Today, vertical movement of the San Andreas Fault system continues to uplift this landscape.

While tectonics has played an important part of the genesis of these cliffs, the effects of winter storms far outpace periodic seismic events when considering decadal geomorphologic change. Observations of coastal cliff landslides have been made during both large and small earthquakes in 1906 (Lawson, 1908), 1957 (Bonilla, 1959), 1989 (Plant & Griggs, 1990, Sitar, 1991) and 2002 (Collins & Sitar, 2002), however, there has been far greater recorded crest retreat and landslide frequency as a result of winter storms (Collins, 2004).

The wave and storm climate of the area is typical of the northern Pacific coast of the United States and generally consists of a Mediterranean-type climate. Following an extensive dry period during the summer and autumn months, a very active storm season begins in November with increased swells from the northwest followed typically by a series of large storms that descend from the far-north Pacific (Storlazzi & Wingfield, 2005). The result is a very wet winter and spring with an average of nearly 470 mm of precipitation falling between the beginning of November and the end of May (NWS, 2006). The resulting connection between precipitation and landslides in the San Francisco area has been well documented (e.g. Ellen & Wieczorek, 1988; Godt, 1999) and the Pacifica area is no exception.

Winter storms also bring periods of high wave action with offshore significant wave heights reaching up to 7.6 meters compared to an annual mean value of 1.8 meters (NOAA/NDBC, 2006). The effect of these storms is to remove built-up sand from the beaches, by up to two meters in some cases (Collins, 2004). This generally exposes the toe of the coastal cliffs to much more severe and more frequent wave action, especially when coupled with high spring-tides (Fig. 1). Wave contact with the cliffs generally occurs at one of the two high tides per day, although during periods of high storm activity, waves may reach the toe even at low tides.

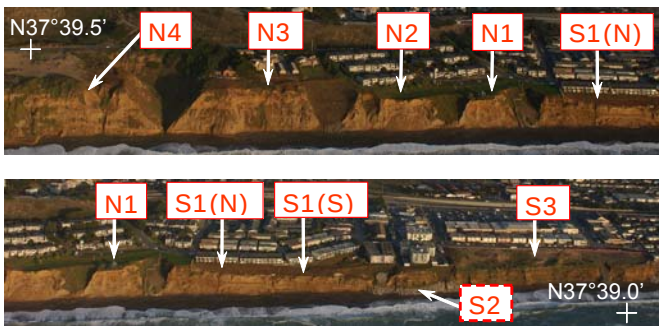

Figure 3. Oblique view of the Pacifica study area showing locations of observed cliffs. Cliff S2 was not observed for failures. Photo courtesy of the California Coastal Records Project.

3 SITE GEOLOGY AND FAILURE MODES

The present study focuses on a 1.5-kilometer length of coast consisting of seven individual cliffs (Fig. 3) reaching an average height of 24 m. Geologic mapping of the area has shown that the northern half of the study area (Cliffs N4, N3, N2, N1 and S1-North) consists of weakly cemented sands while the southern half (Cliffs S1-South and S3) are composed of moderately cemented sands (Collins, 2004). The sand units can be distinguished from one another qualitatively by a field test of slope inclination or quantitatively by unconfined compressive strength (UCS). In general, units with slopes of more than 70° are moderately cemented, whereas slopes less than this are weakly cemented. Geotechnical testing indicates that moderately cemented materials exhibit UCS of up to 400 kPa, with weakly cemented units falling in the 5 to 30 kPa range, consistent with categorical divisions for cemented sands developed by Shafii-Rad & Clough (1982).

Our detailed observations have also shown the predominant failure mode (translative shear failure or tensile-induced topples) as well as the failure mechanism (wave action or precipitation induced seepage) are almost wholly dependent on the lithology of the cliff. In the weakly cemented cliffs, the primary mode of failure is through geometrically constrained, translational shear as a result of wave action (Fig. 4). Early season winter storms with long period energy remove sand from the fronting beach and a combination of high tide and wave run-up allows sea levels to contact the cliff toe. Wave erosion leads to the development of vertical cliff profiles up to several meters in height at the toe, which become unstable from the cliff materials low shear strength (Collins & Sitar, 2005).

In the moderately cemented cliffs, the failure mode is through tensile exfoliation of the outer cliff face from precipitation induced seepage and wetting (Fig. 5). In these materials, the tensile strength is reduced by wetting and subsequent saturation and the cliff face, existing in a state of quasi-stable tension, collapses (Collins & Sitar, 2005). Our observations, laboratory testing, and analyses show that a near-complete state of saturation is necessary for failure, and given the low permeability of the more heavily cemented sand units, that saturation requires a period of significant wetting.

4 METHODOLOGY

We combined a program of regimented site specific monitoring for new cliff failures with high frequency tide, offshore wave height, and precipitation data to identify triggering conditions of coastal cliff failures. We then developed empirical relationships

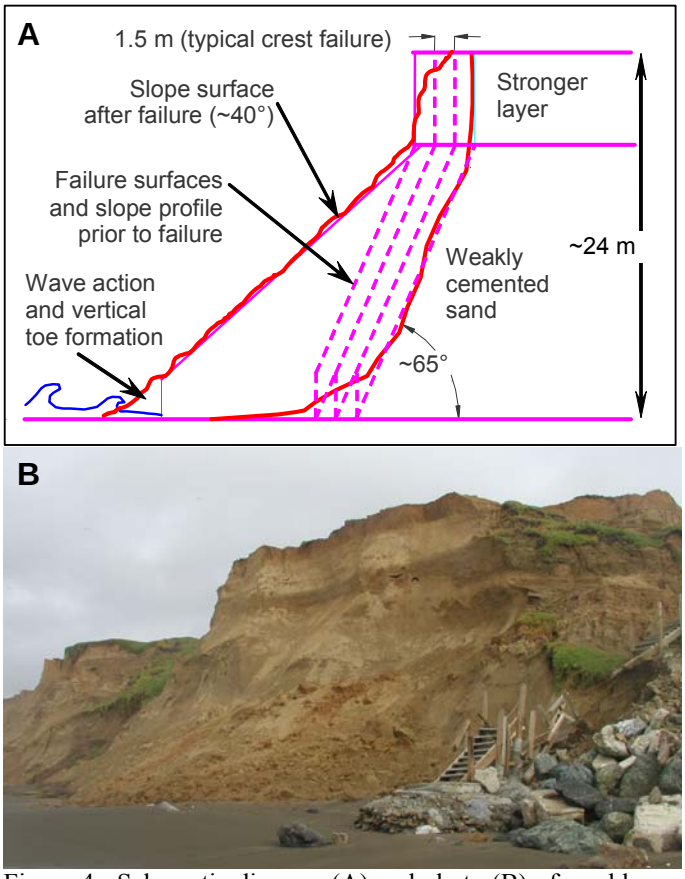

Figure 4. Schematic diagram (A) and photo (B) of weakly cemented coastal cliff failure mode. The failure surface is typically inclined at 65° to the horizontal.

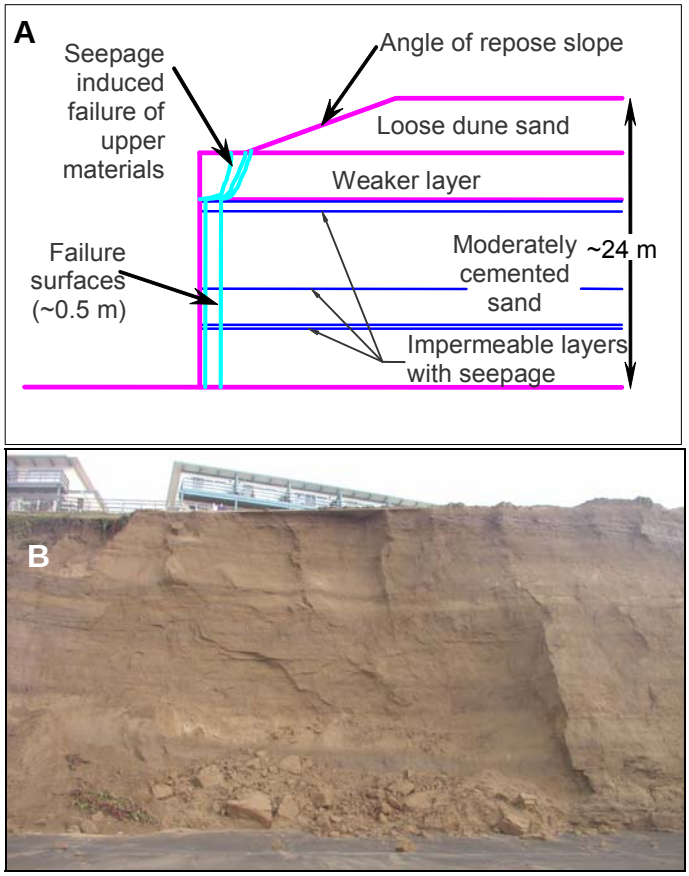

Figure 5. Schematic diagram (A) and photo (B) of moderately cemented coastal cliff failure mode. The failure surface is typically near-vertical.

based on a general implementation of precipitation and wave climate proxies for determining intensity and duration thresholds for each failure mechanism.

4.1 *Monitoring and Observations of Failures*

The coastal cliff monitoring program consisted of direct observations and digital, oblique photography of the study area cliffs. Observations for evidence of failures were made of the seven study area cliffs (Fig. 3) through daily, weekly and monthly field visits to the study area during the 2001-2006 winter storm seasons (November to May). Cliff S1 was divided into north and south sections due to its length and the change in material properties that occurs moving from north to south. Cliff S2 is protected by slope grading and a 4.5 meter tall riprap seawall and was not observed for native failure mechanisms.

Observations were made during low tide to take photographs from the beach looking at the cliffs head on. In total, 128 visits were made during the five winter seasons from 2001-02 to 2005-06. Visits consisted of walking the length of the beach in front of the cliffs and along their crest to document any changes compared with previous visits. Photographs and detailed descriptions of failures were noted on each occasion. When a failure was observed, the probable failure mechanism was determined based directly on field observations of the failure mode and the wave and climate conditions that had occurred since the last field visit. Observed failures for each of the five winter seasons investigated are plotted individually in Figure 6. While an attempt was made to document the occurrence of all failures, the primary effort was directed to identifying those failures that produced crest retreat. A majority of the cliff dataset is available for viewing at http://eriksson.gisc.berkeley.edu/bluff.

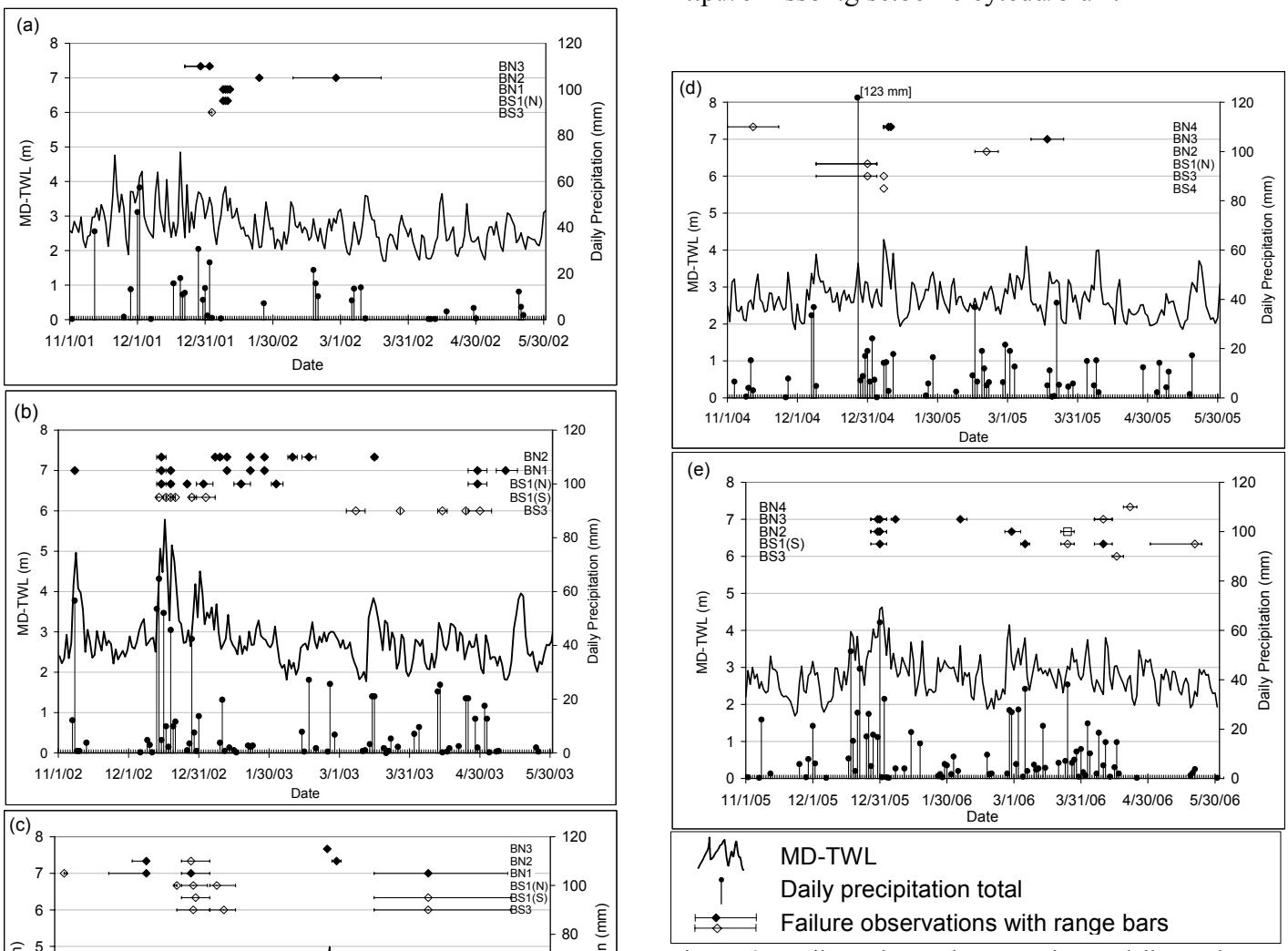

Figure 6. Failure observations, maximum daily total water level, and daily precipitation for the (a) 2001-02, (b) 2002-03, (c) 2003-04, (d) 2004-05, and (e) 2005-06 winter storm seasons. Failure observations with a closed symbol are wave action induced failures; open symbols are precipitation induced failures. Location of symbols within range bars indicate the best approximation of the time of failure within the time period in which failure may have occurred.

4.2 *Failure Event Indicators*

Statistical correlations of observed failures were developed through processed-based indicators of wave action and precipitation. To estimate levels of relative wave climate, we utilized the methodology outlined by Komar (1998) for calculating the relative sea-level elevation on the beach from tides and wave run-up. This provided a measure of the maximum wave run-up level during each of the winter seasons when failures were observed.

The methodology sums the recorded tide level with a measure of wave run-up. We utilized local data from the nearest open-ocean tide gauge located in Point Reyes, California, to the north of the city of Pacifica (NOAA/NOS, 2006). This tide level (η) takes into account both astronomical tide changes and storm surge related anomalies. Wave run-up was measured indirectly, through an empirical correlation developed by Ruggiero et al (2001) for similarly dissipative beaches along the Oregon, USA coast, and which links the deep water significant wave height (H_s) with the wave run-up component. Ruggiero et al's formulation predicts the vertical level exceeded by 2% of the run-up heights ($R_{2\%}$), which gives a measure of the maximum exceedence, suitable for investigating wave conditions leading to cliff failure. The complete wave run-up equation defining the total water level (R) is:

$$R = \eta + R_{2\%} \quad (1)$$

where

$$R_{2\%} = 0.5H_s\text{-}0.22 \quad (2)$$

Since both tide and wave height data were available on an hourly basis, we calculate the maximum daily total water level (MD-TWL) as an indication of wave conditions capable of leading to cliff failure. The resulting maximum daily total water level is plotted for each of the five winter seasons in Figure 6 and seasonal maximums and averages are reported in Table 1. Complete details of the specific methodology used in developing these data sets is available in Collins (2004).

In the moderately cemented cliffs, we observed that high levels of precipitation typically occurred immediately prior to a failure event. Therefore, we utilized daily precipitation records as an indicator of failure conditions. Daily precipitation data were obtained from a nearby rain gauge located 4 km from the study area (NWS, 2006) and are plotted for each of the winter seasons in Figure 6. Seasonal cumulative totals and the maximum total 48-hour precipitation events are reported in Table 1.

Table 1. Seasonal comparison of wave climate and precipitation data.

Winter season	TWL season average (m)	Maximum season TWL (m)	Cumulative season precip. (mm)	Maximum 48-hr precip. event (mm)
2001-02	2.7	4.9	416	104
2002-03	2.8	5.8	729	118
2003-04	2.6	5.0	540	68
2004-05	2.7	4.3	728	130
2005-06	2.8	4.6	846	80

4.3 *Failure Event Correlations*

From the data presented in Figure 6, parameter sets were developed that capture the main characteristics of each failure mechanism. For wave action, our understanding of the failure mode indicates that failure is dependent on the occurrence of a high relative sea-level on the beach (R) and a preliminary early season time period of high wave energy. Thus, the MD-TWL data were used directly as an indicator of waves sufficiently strong to make contact and erode the cliff toe: a measure of wave action intensity.

Our observations also indicated that the beach must be at a lowered elevation to allow high tides and strong wave action to make cliff contact. Since the beach elevation is lowered in the early season (November-December), and builds back up in the late season (April-May), we developed a wave interaction duration parameter to act as a proxy for season-wide wave effects. This parameter, the cumulative difference between the MD-TWL and the average MD-TWL ($\Sigma_{\Delta MD\text{-}TWL}$)for an individual season is defined as:

$$\sum_{\Delta MD-TWL} = \sum_{i=1}^{Nov-May} \left[(MD\ TWL)_i - \left(\frac{\sum_{i=1}^{Nov-May}}{\#days} \right) \right] \quad (3)$$

This parameter provides a trend that begins low or negative, quickly increases to higher positive values in the early-middle portion of the storm season, and then slowly declines in the middle to late season (Fig. 7). In developing this parameter, each season's average and cumulative exceedence is calculated separately since beach and wave climate vary from year to year, and cliff failure conditions are dependent on the individual season climate. The data in Figure 7 show the difference between a winter season with a very active early to middle season (2002-2003) and a season with a less active early season, and only minimally active mid-season (2004-2005).

Parameter sets developed for identifying proxies for precipitation induced failures were more straightforward. We utilized the daily, 48-hour precipitation total as a measure of precipitation intensity, summing the daily readings from consecutive 24-hour periods. Likewise, we used the cumulative season precipitation coinciding with each 48-hour total as a measure of season-wide duration.

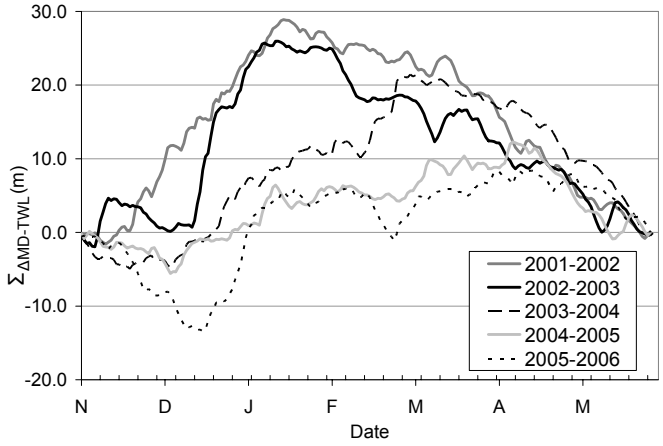

Figure 7. Plot of cumulative difference of maximum daily total water level ($\Sigma_{\Delta MD\text{-}TWL}$) from the season average for each of the 2001-2006 winter seasons.

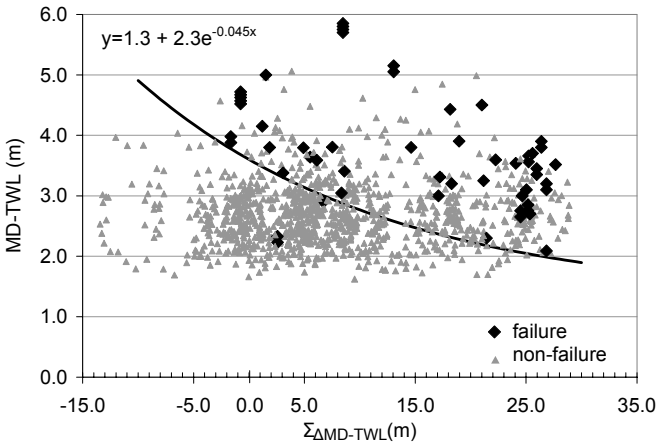

Figure 8. Failure correlation of weakly cemented cliffs with wave action. Failures are predicted to occur in the area above the trend line.

5 RESULTS

5.1 *Wave Action Failure Mechanism*

Plots of each days MD-TWL and cumulative MD-TWL difference from the season average ($\Sigma_{\Delta MD\text{-}TWL}$) for all five storm seasons are shown in Figure 8 along with the associated values for each observed failure outlined in Figure 6. Of note, is the large number of points spread about the mean cumulative difference value of 0.0, indicating that most daily values do not significantly exceed the mean. When the mean is exceeded, it is for a short period of time, as verified by the lower density of points in the upper values (greater than 15 m). It is in this region that many of the days with associated failure events lie.

Due to the observable decrease in the intensity parameter of the failure events with increasing $\Sigma_{\Delta MD\text{-}TWL}$, an exponential function was best fit directly to the data to establish a threshold for failure. The equation:

$$y = 1.3 + 2.3e^{-0.045x} \quad (4)$$

is plotted in Figure 8 and captures almost 95% of the failure events, each located above the threshold. The threshold indicates that periods of wave climate exhibiting extremely high MD-TWL fail under most any beach condition, but that lower levels of MD-TWL require a sufficiently lowered beach condition, quantified by the $\Sigma_{\Delta MD\text{-}TWL}$ parameter.

5.2 *Precipitation Failure Mechanism*

The daily 48-hour precipitation total, along with the associated cumulative season precipitation for each day with a non-zero 48-hour total is plotted in Figure 9. An exponential equation was fit to the data to delineate the precipitation parameter sets that result in failure from those that do not. The equation of this curve is:

$$y = 5 + 20000e^{-0.025x} \quad (5)$$

where y is the daily 48 hour precipitation total and x is the cumulative season precipitation coinciding with the specified 48-hour total. We selected an exponential function to model the physical reality inherent in the data set. That is, with increasing cumulative precipitation, failures occur with much lower 48-hour precipitation totals although a minimum threshold of 5 to 20 mm is still required. Likewise, the function also captures the behavior and requirement of cliff saturation for failure. An antecedent rainfall threshold is indicated by the correlation, requiring at least 200 to 250 mm of seasonal rainfall before failures occur. While some failure data points do not fit the model equation, this is expected given the inherent variability and multi-dependent conditions under which coastal cliff failures occur. However the correlation equation does fit 82% of the failure data points above the model threshold.

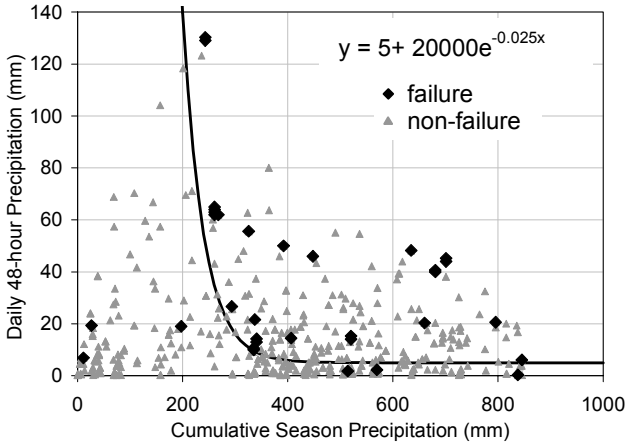

Figure 9. Failure correlation of moderately cemented cliffs with precipitation. Failures are predicted to occur in the area above the trend line.

6 DISCUSSION

The data and results presented in Figures 6-9 allow us to make both short- and long-term predictions of the likelihood of coastal cliff landslides within the study area. Short-term (1 to 5 year) predictions are based on the assumption that the current wave and storm climate, along with the frequency of failures, will follow similar patterns as that observed during the 2001-2006 time period. We base our long-term (decadal) predictions, on the other hand, on the results of state-of-the-art climate model predictions developed specifically for the California coastline.

6.1 *Short-term Failure Predictions – Wave Action*

Short-term predictions of the continuing effects of wave action on the weakly cemented cliffs in the Pacifica study area are made using a single-parameter threshold and a dual-parameter, intensity-duration threshold. We find from the data presented in Figure 6 that the average MD-TWL for all wave action induced failures to be 3.7 m, which is significantly above the average MD-TWL of 2.7 m for all seasons, and also well above the 1σ level (2.7 + 0.6 = 3.3 m). Therefore, we establish a 3.7 m MD-TWL predictive failure threshold, with a strong likelihood of cliff failure when the effects of tide and wave action reach this level.

We move one step further by utilizing the results presented in Figure 8, which show that given a two-parameter estimate of measures of wave action intensity and early season beach erosion duration, that failures are likely when a specific day's parameters plot above the curve defined by Equation 4. For the five season time period from 2001-2006, 434 MD-TWL values exceeded this threshold (Eq. 4) out of a possible 1061 days or approximately 40.9% of the time. Likewise, failures occurred on 52 of these days, which represents 12.0% of the exceedence days or 4.9% of the entire season. We therefore restate these values as predictions: wave action induced failures occur in the study area approximately 5% of the time during the winter storm season, and 12% of the time in which the MD-TWL exceeds the Equation 4 threshold.

6.2 *Short-term Failure Predictions - Precipitation*

Short-term predictions of failure of the moderately cemented cliffs from a precipitation mechanism were developed following the same methodology as for the wave action failure mechanism in the weakly cemented cliffs. Here, we used the daily total precipitation to form a single parameter prediction of failure conditions. From Figure 6, the average 48-hour precipitation event total for all failures resulting from precipitation is 36 mm. This is roughly double the average precipitation event of 15 mm for all five seasons and just above the 1σ level (15 + 18 = 33 mm). We therefore define a 40 mm precipitation event as a threshold level for precipitation induced failures in the moderately cemented cliffs.

The results from Figure 9 allow development of a two-parameter prediction based on the proxies of rainfall intensity and duration as measured by the 48-hour cumulative event total and the coinciding seasonal cumulative total. Here, we define a high likelihood of failure when these parameters plot above the threshold defined by Equation 5. Note that values for the season only represent those days with a 48-hour precipitation value, days without rain are not plotted. During the five seasons investigated, there were 181 days out of a total of 444 days, with precipitation parameters plotting above the threshold. Of these, 27 resulted in failure. Thus, the possibility of failure occurred 40.8% of the time during the season's precipitation days, and failure occurred 6.1% of this time. Of the occurrences plotting above the threshold, failure occurred on 14.9% of these days. We therefore state a short-term prediction of these precipitation induced failures as occurring on roughly 6% of the winter season days with a non-zero 48 hour precipitation value, and approximately 15% of the time that the precipitation parameters plot above the failure threshold defined by Equation 5.

6.3 *Implications of Global Warming on Climate in California*

Long-term predictions of continued cliff failure along the California coast depend on projected climate conditions during the next 100 years. We utilized several recently published reports by the California Climate Change Center (CCCC, 2006a, b, c) which was tasked by the California state government to perform and publish research on the implications of global warming on California's climate. The CCCC used three state-of-the-art global climate models to provide estimates of climate effects for three greenhouse gas emission scenarios. The greenhouse gas scenarios were: B1 - low emissions with high economic growth and stable population but less dependence on fossil fuels, A2 - medium-high emissions with uneven economic growth and continuous population growth with triple the CO_2 concentration relative to pre-industrial levels, and A1fi – high emissions with high fossil fuel dependent economic growth, a peaking - then declining population, and with more than triple the CO_2 concentration compared to pre-industrial levels (CCCC, 2006a).

Our long-term predictions for coastal cliff landsliding are based on the reported results from this body of research and used their estimates of sea-level rise, increased activity in oceanic wave climate, and new precipitation scenarios to model these

effects on the observed failure mechanisms of the Pacifica study area cliffs.

6.4 *Long-term Failure Predictions - Wave Action*

Predictions of the long-term effect of climate change on coastal cliffs affected by wave action were investigated by incorporating results from the CCCC reports on relative changes in future sea level that may occur from greenhouse gas emission driven global warming (CCCC, 2006b). We incorporated only one of the major findings of the report detailing the probable local rise of sea level along the California coast. While the CCCC report also makes clear predictions of a more active wave climate in the northern Pacific Ocean as a result of global warming and an increase in extreme wave heights from a positive shift of the El Niño Southern Oscillation (ENSO) index, we did not incorporate those finding here. However, we do point out that an increase in wave action and extreme sea level events will unquestionably result in a greater quantity and higher frequency of cliff failures.

During the next 70 to 100 years, the CCCC model simulations project that sea level will rise, relative to the year 2000 sea level, by 11-54 cm using the B1 greenhouse gas emission scenario, by 14-61 cm using the A2 scenario, and by 17-72 cm using the A1fi scenario (CCCC, 2006b). For comparison, the report shows that the historic sea-level rise for the past century has been 19.3 cm/century in the San Francisco, California region. Thus, the average and higher bounds of the simulated ranges are a significant increase over recent historic levels.

The effect of a rising sea level trend on coastal cliff landslides was investigated by directly imposing a uniform sea level trend to the 2001-2006 winter season data sets and calculating the number of days that would result in cliff failure. We calculated this value assuming that the ratio between the number of failures and the number of points exceeding the failure threshold remains constant at 12% based on the 2001-2006 data:

$$\frac{\#_{days\ with\ failures}}{\#_{days\ exceeding\ threshold}} = \text{constant} = 12\% \qquad (6)$$

This assumption takes into account the inherent variability of the timing and occurrence of events while also allowing future projected wave action parameters to be evaluated using the established threshold (Eq. 4). As an example, for a projected sea level rise trend of 60 cm in Figure 10, the wave parameters are shifted upwards and to the right compared with Figure 8. The Equation 4 threshold is exceeded on 675 occasions and the number of days where failure is likely to occur increases to approximately 30 additional events from 52 to 81

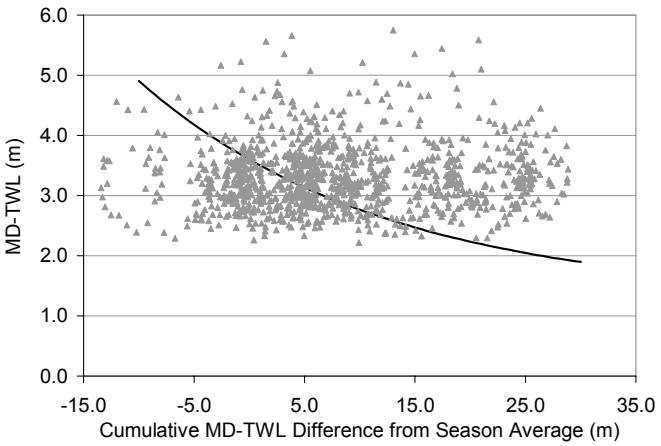

Figure 10. Prediction of wave parameters for a 5 year time period in 100 years with sea-level rise trend of 60 cm imposed on 2001-2006 season data set. Equation 4 failure threshold is plotted for comparison.

events. (Table 2). Predictions of failure events for various additional trends in sea level coinciding with the CCCC greenhouse gas scenarios are outlined in Table 2. With an average level of cliff retreat during a single failure event on the order of 0.5 to 1.5 meters (Collins, 2004), we can make clear predictions that the failure rate and cliff retreat rate will increase in the future given any trend of sea level rise.

Table 2. Prediction of failure events for a 5-year period in 100 years based only on sea level trend.

Sea level trend (m/100yr)	# points exceeding threshold	# days of predicted failure	% increase of failure	Global emissions scenario
0	434	52	0	sea level decline
0.2	506	61	17	present rate
0.4	594	71	37	A2 average
0.6	675	81	56	A2 maximum
0.72	719	86	65	A1fi maximum

6.5 *Long-term Failure Predictions - Precipitation*

According to the CCCC report on Climate Scenarios for California (CCCC, 2006c) the climate model scenarios do not predict any clear trend for the long-term effects of emissions-based climate change on precipitation. In general, the report states that California is likely to maintain its present Mediterranean-style climate, with winter storm seasons bringing the majority of the annual precipitation. The report states that little change in annual precipitation totals are predicted, with only slightly wetter winters and reciprocal drier spring conditions.

The effect of this scenario on the long-term failure rate of the Pacifica coastal cliffs is therefore evident. Based on the CCCC's reports conclusions, we do not expect precipitation induced failures to either increase or decrease during the next 100 years.

It is potentially important, however, to understand how our predictive formulation would behave under wetter or dryer precipitation scenarios. Using Figure

9 as a baseline, under a wetter climate scenario, the cumulative season precipitation level will increase, which will locate more of the season-wide data points to the right within the figure. In this case, the delineating trend line for failure/no-failure remains in the same position, and the likelihood of more days being located above the threshold will increase. With higher single day precipitation totals, the effect will be similar, with the parameters for more days moving upwards in the figure, and likewise a higher chance for failure with more days plotted above the failure threshold. Under a dryer climate scenario, the reverse will be true for each of these parameters: the data points will move down and to the left in Figure 9, and there will be less likelihood for failure from this mechanism.

7 CONCLUSIONS

Coastal cliff failures in weakly lithified sediments are an inevitability in most coastal settings around the world and we have shown that the cliffs located south of San Francisco, California are no exception. Detailed observations and wave and precipitation data sets collected over a five season time period from 2001-2006 have shown that empirical correlations that predict distinct failure thresholds can be identified (Eqs. 4-5). We identified these thresholds for the two predominant failure modes that occur in the study area: wave action induced translative shear failure in weakly cemented sand cliffs and precipitation driven seepage and tensile failure in moderately cemented sand cliffs. The thresholds were calculated as exponential functions, consistent with a processed based understanding of higher failure thresholds when intensity parameters are high and duration parameters are low, and lower failure thresholds with the reverse case.

The correlation equations also provide starting points for carrying out forecasting analyses aimed at understanding the impact of future trends in sea-level, wave action, and precipitation events. Given the current understanding of the effect of increased greenhouse gas emissions to global warming and state-of-the-art climate model predictions, we project an increase in wave action driven failures of the weakly cemented cliffs, potentially reaching over 165% of the current number of failures per year. This represents an increase from 52 failures per 5-year period measured during the 2001-2006 winter seasons to 86 failures per 5-year period for a sea level trend consistent with a high greenhouse gas emissions (A1fi) scenario. Obviously, other scenarios are also possible. On the other hand, we predict a constant level of precipitation-induced failures in the moderately cemented cliffs of the Pacifica study area consistent with current and projected levels of precipitation.

Future work in this area will be aimed at incorporating the effect of sea level extremes and wave height anomalies into our future predictions of wave driven failures in the weakly cemented cliffs in the study area. We also intend to model wave action more rigorously by incorporating the effects of short and long period waves on either removing or accreting sand to the beach - an issue tied directly into the proper modeling of the failure threshold duration parameter.

8 ACKNOWLEDGEMENTS

Funding for this research was provided by the U.S. Geological Survey, Mendenhall Postdoctoral Research Program, the U.S. Geological Survey, Western Coastal and Marine Geology Program, and the University of California, Coastal Environmental Quality Initiative. Pamela Patrick and Ann Marie Puzio, former graduate students at the University of California, Berkeley were responsible for several years of the data collection phase of this work and their diligence with site visits and observations are gratefully acknowledged. The authors wish to thank Monte Hampton for valuable insights and observations of the study area and Jonathan Allen at Oregon DOGAMI for helpful suggestions to the wave run-up analyses. The photo in Figure 2 is used with permission from Cotton, Shires and Associates and the photos in Figure 3 are used with permission of the California Coastal Records Project.

9 REFERENCES

Bonilla, M.G., 1959, Geologic observation in the epicentral area of the San Francisco earthquake of March 22, 1957., G.B. Oakenshott, ed., *Spec. Rep. 57, California Division of Mines*, pp25-37.

Caine, N., 1980, The rainfall intensity-duration control of shallow landslides and debris flows: *Geografiska Annaler*, Vol. 62A, pp23-27.

Cannon, S.H., 1988, Regional rainfall-threshold conditions for abundant debris-flow activity, *in* Ellen, S.D. and Wieczorek, G.F., eds., Landslides, floods, and marine effects of the storm of January 3-5, 1982, in the San Francisco Bay region, California: *U.S. Geological Survey Professional Paper No. 1434*, pp35-42.

CCCC, 2006a, Our Changing Climate: Assessing the Risks to California, *California Climate Change Center, General Publication, Report No. CEC-500-2006-077*, Prepared by Luers, A.L., Cayan, D., Franco, G., Hanemann, M., and Croes, B. http://www.climatechange.ca.gov/ biennial_reports/ 2006report/index.html, 64p.

CCCC, 2006b, Projecting Future Sea Level, *California Climate Change Center White Paper, Report No. CEC-500-2005-202-SF*, Prepared by Cayan, D., Bromirski, P, Hayhoe, K, Tyree, M, Dettinger, M, and Flick, R., http://www.climatechange.ca.gov/bienial_reports/2006report/index.html, 64p.

CCCC, 2006c, Climate Scenarios for California, California Climate Change Center White Paper, Report No. CEC-500-2005-203-SF, Prepared by Cayan, D., Maurer, E., Dettinger, M., Tyree, M., Hayhoe, K., Bonfils, C, Duffy, P., and Santer, B., http://www.climatechange.ca.gov/biennial_reports/2006report/index.html, 64p.

Cleveland, G.B., 1975, Landsliding in Marine Terrace Terrain, California: *Special Report 119 of the California Division of Mines and Geology*, 24p.

Clough, G.W., Sitar, N., Bachus, R.C, & Shaffii-Rad, N., 1981, Cemented sands under static loading, *ASCE Journal of Geotechnical Engineering*, Vol. 107(GT6), June 1981, pp. 799-817.

Collins, B.D., 2004. *Failure Mechanics of Weakly Lithified Sand Coastal Bluff Deposits*: Doctoral dissertation, University of California, Berkeley, 278p.

Collins, B.D. & Sitar, N., 2002. Geotechnical Observations of Recent Coastal Bluff Failures, Pacifica, California, *Geological Society of America - 98th Cordilleran Section Annual Meeting, Corvallis, Oregon, May 13–15, 2002*.

Collins, B.D. & Sitar, N., 2005. Failure mode identification and hazard quantification for coastal bluff landslides, *Proceedings 2005 International Conference on Landslide Risk Management*, Eds. O. Hungr, R. Fell, R. Couture, & E. Eberhardt, Vancouver, BC, Canada, June 2005, pp. 487-496.

Ellen, S.D. & Wieczorek, G.F., 1988. Landslides, floods, and marine effects of the storm of January 3-5, 1982 in the San Francisco Bay region. *U.S. Geological Survey Professional Paper 1434*: 310p.

Godt, J.W., 1999. Maps showing locations of damaging landslides caused by El Niño rainstorms, winter season 1997-98, San Francisco Bay region, California, J.W. Godt, ed., *U.S. Geological Survey Miscellaneous Field Studies Maps MF-2325-A-J*.

Hampton, M., 2002, Gravitational failure of sea cliffs in weakly lithified sediment: *Environmental and Engineering Geoscience*, Vol. 8(3), pp175-192.

Hampton, M. & Dingler, J., 1998, Short term evolution of three coastal cliffs in San Mateo County, California: *Shore and Beach*, Vol. 66(4), pp. 24-30.

Komar, P. D. (1998). Beach Processes and Sedimentation, Prentice Hall, New Jersey.

Lajoie, K. R. & Mathieson, S. A., 1998, 1982-83 El Niño Coastal Erosion, San Mateo County, CA: *U.S. Geologic Survey Open-File Report 98-041*, 61p.

Lawson, A.C. (1908). The California earthquake of April 18, 1906, *Publication No. 87, Report of the State Earthquake Investigation Commission*. Vol. 1, 451p.

Nilsen, T.H., Taylor, F.A., & Dean, R.M., 1976, Natural conditions that control landsliding in the San Francisco Bay region – an analysis based on data from the 1968-69 and 1972-73 rainy seasons: *U.S. Geological Survey Bulletin 1424*, 35p.

NOAA/NDBC, 2006, National Oceanic and Atmospheric Association, National Data Buoy Center (online), <http://www.ndbc.noaa.gov/>, Site #46026, San Francisco, California.

NOAA/NOS, 2006, National Oceanic and Atmospheric Association, National Ocean Service Observed Water Levels and Associated Ancillary Data (online), http://co-ops.nos.noaa.gov/data res.html, Site #9415020, Point Reyes, California.

NWS, 2006, National Weather Service Forecast Office, San Francisco Bay Area/Monterey (online), <http://www.wrh.noaa.gov/Monterey/rtp02/>, Site # Pacifica 2S, Pacifica, California (PCAC1).

Plant, N. & Griggs, G.B., 1990, Coastal landslides caused by the October 17, 1989 earthquake, *California Geology*, Vol.43(4), p75-84.

Ruggiero, P., Komar, P. D., McDougal, W. G., Marra, J. J., & Beach, R. A. (2001). "Wave Runup, Extreme Water Levels and the Erosion of Properties Backing Beaches." *Journal of Coastal Research*, 17(2), 407-419.

Sallenger, A.H., Krabill, W., Brock, J., Swift, R., Manizade, S. & Stockdon, H., 2002, Sea-cliff erosion as a function of beach changes and extreme wave run-up during the 1997-1998 El Niño: *Marine Geology*, Vol. 187, pp. 279-297.

Shafii-Rad, N. & Clough, G.W. 1982, The Influence of Cementation on the Static and Dynamic Behavior of Sands: *John A. Blume Earthquake Engineering Center, Report No. 59, Stanford University, California, December 1982*, 315p.

Sitar, N., 1983. Slope stability in coarse sediments, *ASCE Special Pub.: Geologic Environment and Soil Properties*, R.N. Yong, ed., pp. 82-98.

Sitar, N., 1991, Earthquake-induced landslides in coastal bluffs and marine terrace deposits, *Spec. Pub. No. 1, Loma Prieta Earthquake, Ass. of Eng. Geology*, pp67-82.

Snell, C. B., Lajoie, K.R. & Medley, E. W., 2000, Sea-Cliff Erosion at Pacifica, California Caused by the 1997/98 El Niño Storms: *Slope Stability 2000, ASCE Geot. Spec. Pub. No. 101, Proc. of Geo-Denver, Denver, Colorado*, August 5-8, 2000, pp. 294-308.

Storlazzi, C.D. and Wingfield, D.K, 2005, Spatial and temporal variations in oceanographic and meteorologic forcing along Central California:1980-2002: *U.S. Geological Survey Scientific Investigations Report 2005-5085*, 30 pp.